International Journal of Innovative Research in Engineering & Management (IJIREM)
ISSN: 2350-0557, Volume-9, Issue-5, October 2022
https://doi.org/10.55524/ijirem.2022.9.5.1
Article ID IJIRD-1199, Pages 1-10
www.ijirem.org

Analysis of the Effects of Renewable Energy-Distributed Generation in a Distribution Network

Mgbeike V. O[1], Ezechukwu O. A[2], Ezendiokwelu C. E[3], and Nwoye A. N[4]

[1,2,3,4,] Department of Electrical Engineering, Nnamdi Azikiwe University Awka, Anambra State, Nigeria

Correspondence should be addressed to Mgbeike V. O; ce.ezendiokwelu@unizik.edu.ng

ABSTRACT- The increasing implementation of Distributed Generation in power systems has turned the conventional "passive" distribution network into an "active" one. In an active distribution network, some costumers not only consume electricity, but they also generate electricity and if their generation surpasses the power demand, these customers will then supply the excess to the network. Photovoltaic energy penetration in the Nigeria distribution network was modelled using ETAP Software in this work. Short circuit analysis was performed using symmetrical components while the power flow analysis of the network was done using the Newton-Raphson method.

KEYWORDS- Distribution, Generation, Photovoltaic, Power System, Renewable, Tripping.

I. INTRODUCTION

The conventional power system has many subsystems and dynamic elements equipped with control systems to stabilize the overall operation. The prime mover controller is used in power plants to regulate the speed and in effect the active power while the excitation controller regulates the voltage and in effect the reactive power output. The conventional interconnected power system can be envisioned as a single system and for a stable operation it is necessary that all the large synchronous generators remain in synchronism. Instability usually occurs if a power system cannot maintain the voltage levels within a required range (Kroposki et al. 2017). The implementation of distributed generation influences both steady state and dynamic performance of a power system. The possible penetration level of photovoltaic (PV) system into the network which is the most commonly available and widely used distributed generation technologies was investigated in this work. It is always advisable for any electrical network that the voltage, frequency, and current should not increase beyond a limit for the general safety, and to avoid the damage of different types of equipment connected with the network. The increasing growth of renewable penetration into the distribution network might create an unfavourable effect on the power system network. Therefore it is necessary to think about the problem related with the distributed penetration and the maximum penetration that would not create problem to the electrical power network system. There have been a good number of research works proposing for these renewable energy sources like PV systems to be introduced in the Nigeria distribution network, hence it is desirable to have a good understanding about the impacts due to the DG systems into the Nigeria distribution network. In this paper the effects of distributed renewable penetration into the Umuahia 33kV distribution network in the Nigeria power system was studied.

II. LITERATURE REVIEW

There are different protection schemes which include the distant protection, feeder OC protection scheme e.t.c. The basic principle of distance protection involves the division of the voltage at the relaying point by the measured current. The apparent impedance so calculated is compared with the reach point impedance. If the measured impedance is less than the reach point impedance, it is assumed that a fault exists on the line between the relay and the reach point [2]. The operation of the overcurrent (OC) protection scheme requires that accurate measurement of fault current magnitude, and then comparison with a predefined OC threshold to determine if a fault has occurred. If a fault occurred, then the protection devices must respond in a coordinated manner for fast and selective isolation of the fault anywhere along the feeder and laterals [3], [4]. In [5] a conventional OC protection system was assumed to have unidirectional current flow as well as having a fixed pickup setting determined through load flow study. The feeder OC protection system based on this assumption was designed such that the coordinated switching strategy will be maintained irrespective of change in network condition such as load changes and network topology reconfiguration. The fixed threshold setting based on the location of the protective device was used to ensure that all protective devices including protective relay within a switching strategy were coordinated. An adaptive protection scheme based on dividing the existing distribution networks into zones and maintaining a load balance with the application of emerging technologies for updating of network status has been proposed by [6], [7].

In [8] the challenges of short circuit in radial distribution system at different fault levels during different topologies due to source changes or in some cases completely loss of coordination in the existed protection scheme leads to undesired islanding and untimely tripping of DGs protection relays and a high DG protection has resulted in the possibility of operating distribution system in islanded mode which has an issue in conventional OC protection system and needs a new requirement in the power system protection scheme. In [9] was proposed an adaptive scheme based on changing the pickup setting of the OC relay by estimating the fault current magnitude using an iterative

technique. The speed of convergence of the technique will determine the overall response time of the scheme, and this has not been reported. In [10] an adaptive selection of appropriate relay operating curves based on state estimation technique for faulted section detection as well as detection of fault magnitude under grid connected and island mode. It was demonstrated in [11] an adaptive control strategy of converter based DG to maintain protection coordination in distribution system. The proposed protection strategies based on controlling the inverter interfaced DERs output current under fault conditions by detecting the decrease in voltage at the DERs, thus reducing the fault current contribution by the DERs, hence allowing the OC relay to operate correctly using the existing setting. However, with network topological change the relay preset parameters must be adaptive for this to be effective. Proposed in [12] was another algorithm based on dynamic Thevenin parameter estimation to compute the estimated fault current magnitude for adaptive relay setting. A technique based on recursive discrete Fourier transform for fundamental phasor estimation , and Fuzzy logic controller to set relay trip setting was propsed in [13]. In [14] a technique based on decision-tree to analyse the harmonic current magnitudes; however, this does not perform well under noisy environments. In [15] proposed a technique based on Kalman filter and support vector machine (SVM), which is based on statistical learning theory to extract features of magnitude and frequency of the fundamental and some odd harmonics components. The technique requires large data set for training which can become problematic if good dataset is not available. The changes in fault currents passing through protection devices when DGs are connected to the system was demonstrated and suggested that protection coordination must be checked after connecting each DG to distribution network [16]. However, this approach is applicable only in the presence of low penetration of DGs into the system.

III. MATERIALS AND METHODS

The short circuit current characteristics of DGs and their contribution to fault currents at all buses and branches in various cases were investigated under different control strategies. Load flow analysis and short-circuit fault analysis were conducted to study the effect of DG integration into the power system for different system configurations and fault locations. The Nigeria distribution system was the case study power system and was modelled using ETAP Software with photovoltaic energy used as the DG for this paper. The short circuit analysis was performed using symmetrical components while the power flow analysis of the network was done by Newton-Raphson method.

A. The Newton-Raphson Method

There are several methods of solving the non-linear system of equations. The most efficient one is the Newton-Raphson method. This method begins with initial guesses of all unknown variables such as voltage magnitude and angles at load buses and voltage angle at generator buses. Next, a Taylor series is written for each of the power balance equations included in the system of equations. The result is a linear system of equations that can be expressed as follows:

$$\begin{bmatrix} \Delta\theta \\ |\Delta V| \end{bmatrix} = J^{-1} \quad (3.1)$$

$$\Delta P_i = -P_i + \sum_{k=1}^{n} |V_i|\,|V_k|(G_{ik}\cos\theta_{ik} + B_{ik}\sin\theta_{ik}) \quad (3.2)$$

$$\Delta Q_i = -Q_i + \sum_{k=1}^{n} |V_i|\,|V_k|(G_{ik}\,cos\,\theta_{ik} - B_{ik}\,sin\,\theta_{ik}) \quad (3.3)$$

$$J = \begin{vmatrix} \frac{\partial\Delta P}{\partial\theta} & \frac{\partial\Delta P}{\partial|V|} \\ \frac{\partial\Delta Q}{\partial\theta} & \frac{\partial\Delta Q}{\partial|V|} \end{vmatrix} \quad (3.4)$$

Where $\Delta P\ and\ \Delta Q$ are called the mismatch equations and J is a matrix of partial derivatives known as a Jacobian. The linear system of equation is solved to determine the next guess (m+1) of voltage magnitude and angles based on

$$\theta^{m+1} = \theta^m + \Delta\theta \quad (3.5)$$

$$|V|^{m+1} = |V|^m + \Delta|V| \quad (3.6)$$

The process continues until a stopping condition is met. A common stopping condition is to terminate if the norm of the mismatch equation is below a specified tolerance.

B. Modelling of the Case Power System

The two bus system with the receiving end voltage as a reference phasor is given as $V_R = |V_R| < 0°$ and the sending end voltage lead it by an angle δ given as $V_s = |V_s| < \delta°$, where δ is the torque angle. The complex power leaving the receiving end and entering the sending end of the transmission line can be expressed per phase in equation (3.7) and (3.8) respectively.

Figure 1: Single line diagram of a two bus system

$$S_S = P_S + jQ_S = V_S I_S \quad (3.7)$$

$$S_R = P_R + jQ_R = V_R I_R \quad (3.8)$$

Where I_S, I_R are the sending end and receiving end currents and can be expressed in terms of their sending-end and receiving-end voltages through a transmission line whose equation is given as expressed in eqn (3.9).

$$\begin{bmatrix} V_S \\ I_S \end{bmatrix} = \begin{bmatrix} A & B \\ C & D \end{bmatrix} * \begin{bmatrix} V_R \\ I_R \end{bmatrix} \quad (3.9)$$

And ABCD are the transmission line constraints

S_S = Sending end power Q_R = Receiving end reactive power

S_R = Receiving end power V_S = Sending end Voltage

P_S = Sending end real power V_R = Receiving end Voltage

P_R = Receiving end real power I_S = Sending end current

Q_S = Sending end reactive power I_R = Receiving end current

Hence,

$$I_R = \frac{1}{B}V_S - \frac{A}{B}V_R \quad (3.10)$$

$$I_S = \frac{D}{B}V_S - \frac{I}{B}V_R \quad (3.11)$$

Let A, B, D, the transmission line constants, given in equation (3.9) and (3.10) be;

$A = |A| < \alpha, B = |B| < \beta, D = |D| < \alpha \ (since\ A = D)$

Substituting in equation (3.10) and (3.11), we have equations (3.12) and (3.13) as follows:

$$I_R = \left|\frac{1}{B}\right| * |V_S| < (\delta - \beta) - \left|\frac{A}{B}\right| * |V_R| < (\alpha - \beta) \quad (3.12)$$

$$I_S = \left|\frac{D}{B}\right| * |V_S| < (\alpha + \delta - \beta) - \left|\frac{1}{B}\right| * |V_R| < -\beta \quad (3.13)$$

Substituting in equation (3.12) and (3.13), in equations (3.7) and (3.8), we have

$$S_R = |V_S| < 0 \ \left[\left|\frac{1}{B}\right| * |V_S| < (\delta - \beta) - \left|\frac{A}{B}\right| * |V_R| < (\alpha - \beta)\right] \quad (3.14)$$

$$S_{S=} \left|\frac{D}{B}\right| * |V_S|^2 < (\beta - \alpha) - \left|\frac{[V_S]|V_R|}{B}\right| < (\beta + \alpha) \quad (3.15)$$

Then, three phase receiving-end complex power $S_R$is given by equation (3.16)

$$S_{R(3phase)=} \left|\frac{[V_S]|V_R|}{B}\right| < (\beta - \delta) - \left|\frac{A}{B}\right| * |V_R|^2 < (\beta - \alpha) \quad (3.16)$$

The imaginary parts of equation (3.14) and (3.15) are expressed in equation (3.17) to (3.20)

For receiving end:

$$P_R = \left|\frac{|V_R||V_R|}{B}\right| \cos(\beta - \delta) - \left|\frac{A}{B}\right| * |V_R|^2 \cos(\beta - \alpha) \quad (3.17)$$

$$Q_R = \left|\frac{|V_S||V_R|}{B}\right| \sin(\beta - \delta) - \left|\frac{A}{B}\right| * |V_R|^2 \sin(\beta - \alpha) \quad (3.18)$$

For sending end:

$$P_S = \left|\frac{D}{B}\right| * |V_R|^2\, cos(\beta - \alpha) \left|\frac{|V_S||V_R|}{B}\right| \cos(\beta + \alpha) \quad (3.19)$$

$$Q_S = \left|\frac{D}{B}\right| * |V_S|^2\, sin(\beta - \alpha) \left|\frac{|V_S||V_R|}{B}\right| \sin(\beta + \alpha) \quad (3.20)$$

From the above equations P_R will be maximum when $\beta = \delta$

Such that

$$P_{R(max)} = \left|\frac{|V_S||V_R|}{B}\right| - \left|\frac{A}{B}\right| * |V_R|^2\, cos(\beta - \alpha) \quad (3.21)$$

$$Q_{R(max)} = -\left|\frac{A}{B}\right| * |V_R|^2\, sin(\beta - \alpha) \quad (3.22)$$

Let A,B,C,D the transmission line constants for a short transmission line given as:

$$\begin{vmatrix} A & B \\ C & D \end{vmatrix} = \begin{vmatrix} 1 & Z \\ 0 & 1 \end{vmatrix} \quad (3.23)$$

Let A,B,C,D the transmission line constants for a medium length line (nominal-π model) given as equation (3.24).

$$\begin{vmatrix} A & B \\ C & D \end{vmatrix} = \begin{bmatrix} (1 + \frac{1}{2}YZ) & Z \\ Y(1 + \frac{1}{4}YZ) & (1 + \frac{1}{2}YZ) \end{bmatrix} \quad (3.24)$$

Where Z= total series impedance and Y =total shunt admittance.

The Umuahia transmission system which is the case power system comprises of several buses which are interconnected by means of power lines. Power is injected into a bus from generator while the loads are tapped from it.

Thus at the i^{th} bus, the net complex power injected into the bus is given by equation (3.25)

$$S_i = P_i + jQ_i = (P_{Gi} - P_{Di}) + j(Q_{Gi} - Q_{Di}) \quad (3.25)$$

While the complex power supplied by the generator is given in equation (3.26)

$$S_{Gi} = P_{Gi} + jQG_i \quad (3.26)$$

And the complex power drawn by the load is given in equation (3.27)

$$S_{Di} = P_{Di} + jQ_{Gi} \quad (3.27)$$

The real and reactive powers injected into the i^{th} bus are given by equation (3.28)

$$P_i = P_{Gi} - P_{Di} \quad i = 1,2,3, \dots \dots, n$$
$$Q_i = Q_{Gi} - Q_{Di} \quad i = 1,2,3, \dots \dots, n \quad (3.28)$$

IV. RESULTS AND DISCUSSION

Different cases simulations of the Umuahia distribution network in the Nigeria power system were done; case system without renewable energy DG, with distributed generation and with different levels of distributed generation for faults at various locations. Load flow analysis was done so as to observe the active power, reactive power and bus voltages. The ETAP software was used to simulate three phase faults at various locations in the Umuahia distribution network.

A. ase when Fault was located at Afara 33kV Feeder End without DG

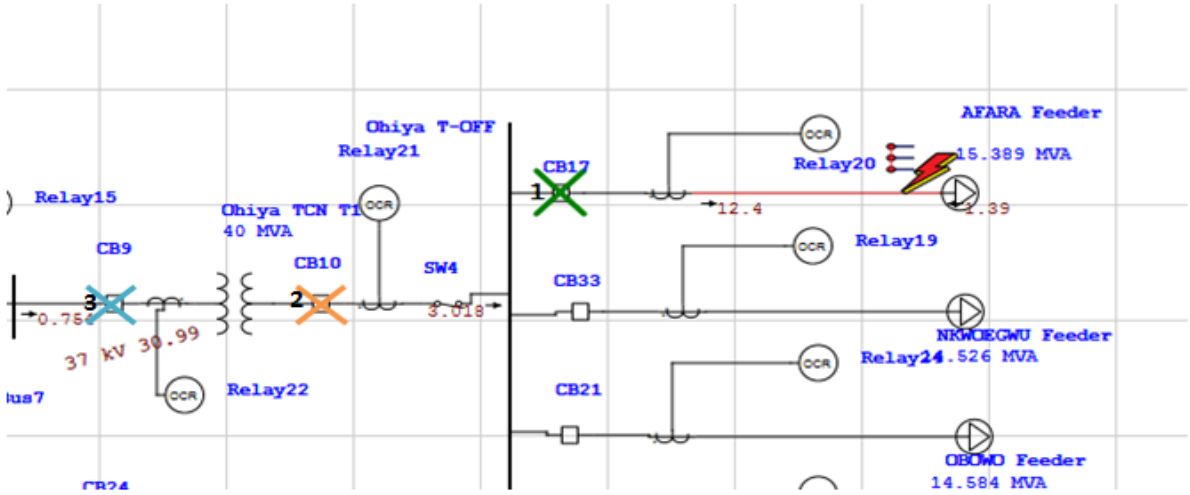

Figure 2: Network diagram for fault located at Afara 33 kV feeder end without DG

Table 1: Sequence of operation summary report for fault at Afara feeder end without DG

Symmetrical 3-Phase Fault at Afara feeder end without DG			
Time (ms)	**ID**	**If (kA)**	**Condition**
10.0	R20	2.550	Phase –OC1 – 50
78.1	R21	2.323	Overload Phase – Thermal
83.3	R22	2.145	Phase – OC1 – 50
310	Afara feeder CB Phase – OC1 – 50		Tripped by R20

B. Relay Coordination Analysis for Fault located at Afara 33kV feeder end with 20% DG Penetration considering islanded mode

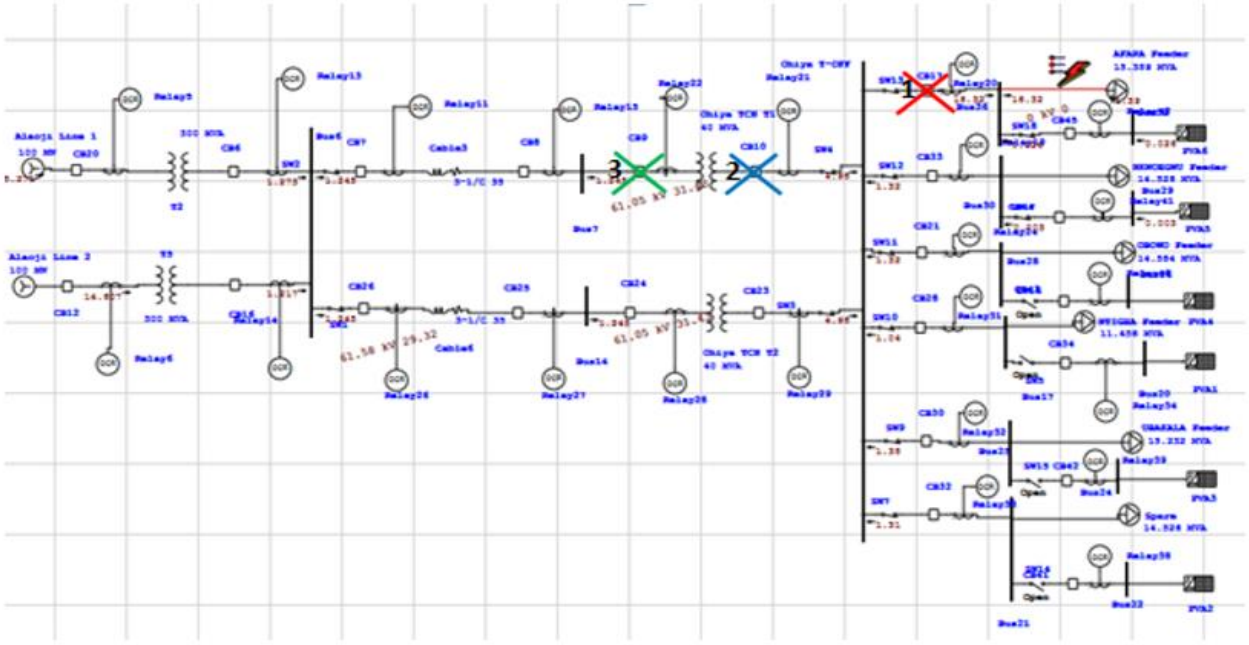

Figure 3: Relay coordination simulation for fault on Afara feeder for 20% DG penetration

Table 2: Sequence of operation summary report with Fault at Afara 33kV feeder for 20% DG Penetration

Symmetrical 3-Phase Fault at Afara 33kV feeder for 20% DG Penetration			
Time (ms)	**ID**	**If (kA)**	**Condition**
11.4	R20	2.695	Phase –OC1 – 50
82.8	R21	2.591	Overload Phase – Thermal
87.7	R22	2.475	Phase – OC1 – 50
337	Afara feeder CB		Tripped by R20 Phase – OC1 – 50
345	CB10		Tripped by R21 Overload Phase
389	T1 CB		Tripped by R22 Phase – OC1 – 50

C. Fault located at Afara 33kV feeder end with 50% DG Penetration

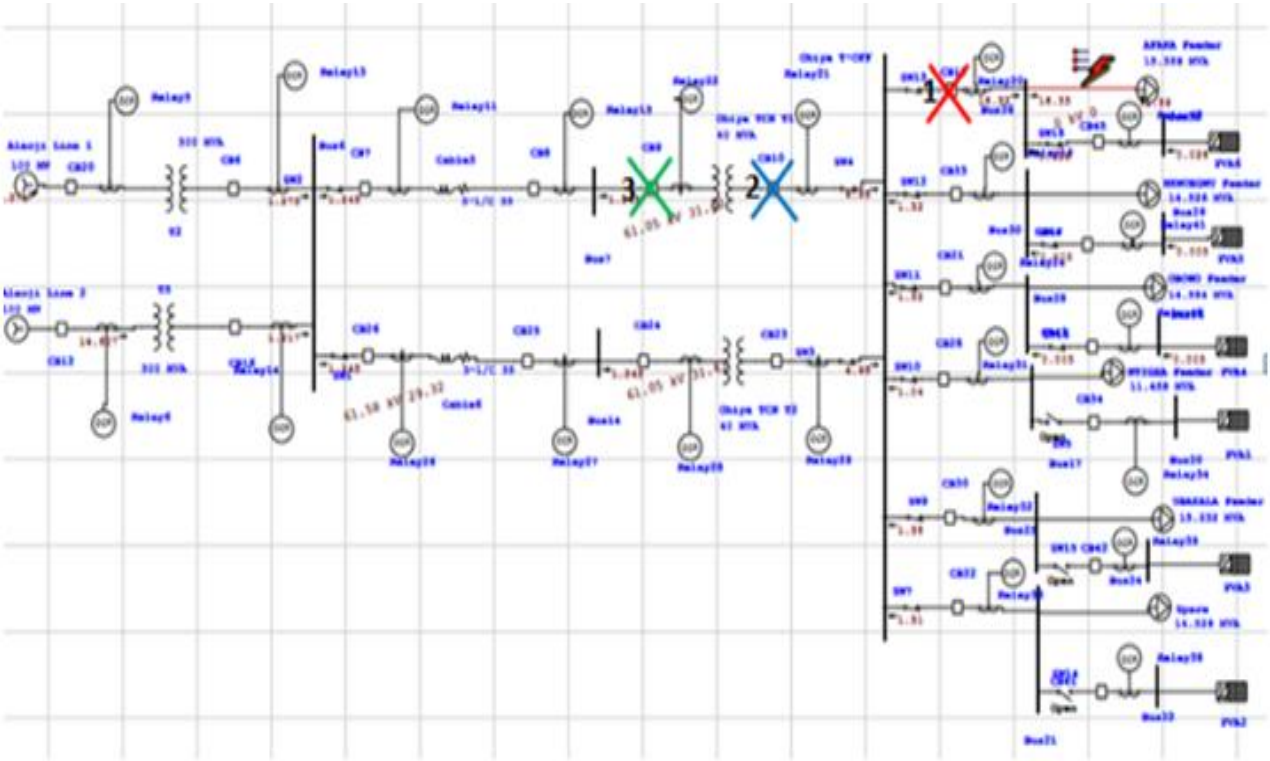

Figure 4: Relay coordination simulation for fault on Afara feeder for 50% DG penetration

Table 3: Sequence of operation event summary report for 50% DG Penetration

Symmetrical 3-Phase Fault at Afara 33kV feeder for 50% DG Penetration			
Time (ms)	**ID**	**If (kA)**	**Condition**
11.3	R20	2.696	Phase –OC1 – 50
82.7	R21	2.592	Overload Phase – Thermal
87.6	R22	2.476	Phase – OC1 – 50
336	Afara feeder CB		Tripped by R20 Phase – OC1 – 50
344	CB10		Tripped by R21 Overload Phase
388	T1 CB		Tripped by R22 Phase – OC1 – 50

D. Fault located at Afara 33kV feeder end with 70% DG Penetration

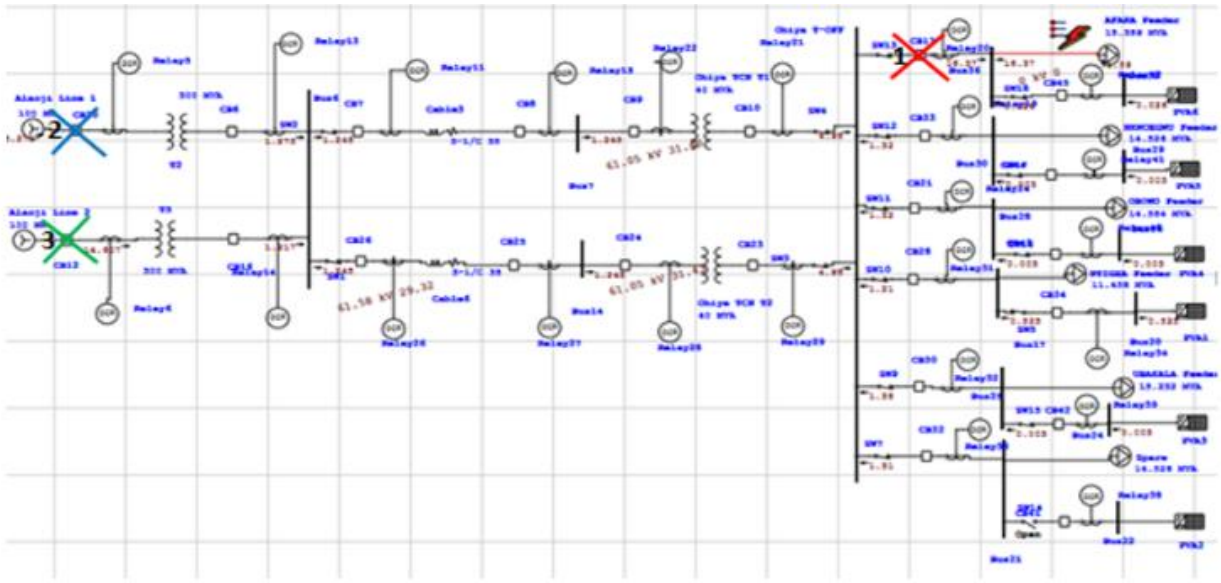

Figure 5: Relay coordination simulation for fault on Afara feeder for 70% DG penetration with Islanded mode

Table 4: Sequence of operation event summary report for 70% DG Penetration

Symmetrical 3-Phase Fault at Afara 33kV feeder for 70% DG Penetration			
Time (ms)	**ID**	**If (kA)**	**Condition**
18.5	R20	1.325	Phase –OC1 – 50
102.3	R5	1.242	Overload Phase – Thermal
107.6	R6	1.135	Phase – OC1 – 50
431	Afara feeder CB		Tripped by R20 Phase – OC1 – 50
429	CB20	1.346	Tripped by R21 Overload Phase
416	CB12	1.349	Tripped by R22 Phase – OC1 – 50

E. Case when fault was located at the 33 kV bus without DG

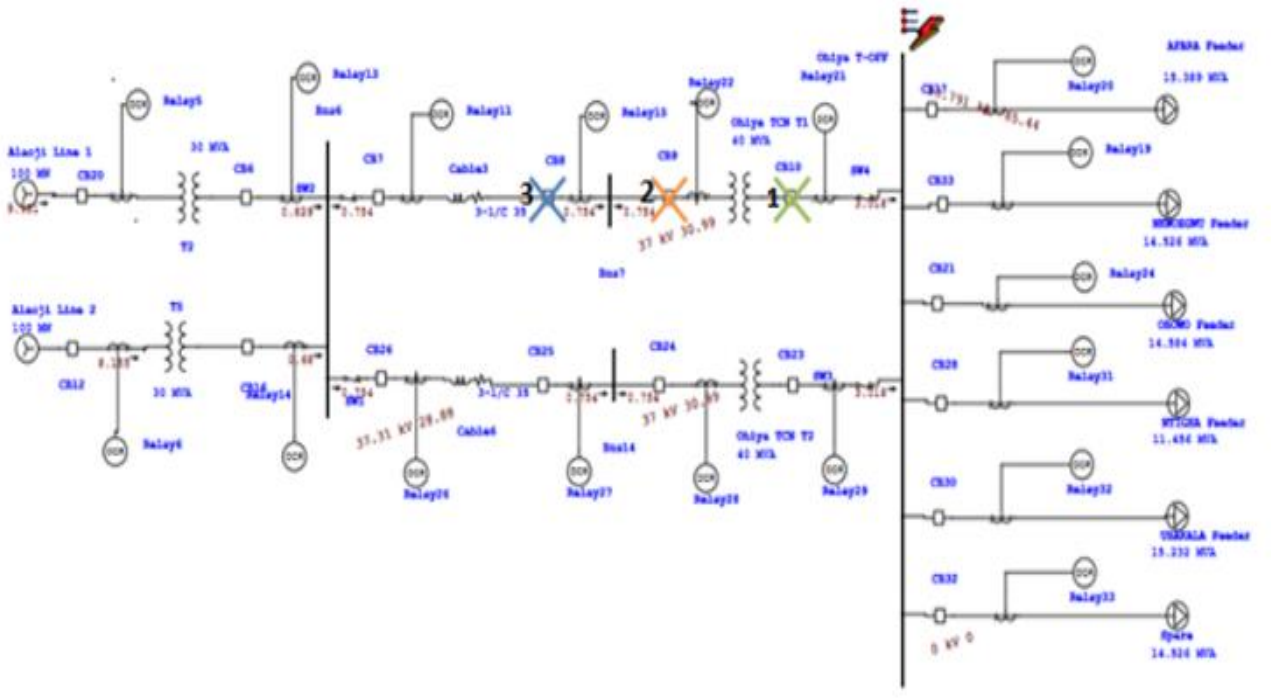

Figure 6: Relay Coordination for fault at 33 kV bus without DG

Table 5: Sequence of operation summary for fault at 33kV bus without DG

Symmetrical 3-Phase Fault at Afara 33kV feeder for 70% DG Penetration			
Time (ms)	**ID**	**If (kA)**	**Condition**
18.5	R20	1.325	Phase –OC1 – 50
102.3	R5	1.242	Overload Phase – Thermal
107.6	R6	1.135	Phase – OC1 – 50
431	Afara feeder CB		Tripped by R20 Phase – OC1 – 50
429	CB20	1.346	Tripped by R21 Overload Phase
416	CB12	1.349	Tripped by R22 Phase – OC1 – 50

F. When fault was located at 33kV bus with 20% DG Penetration

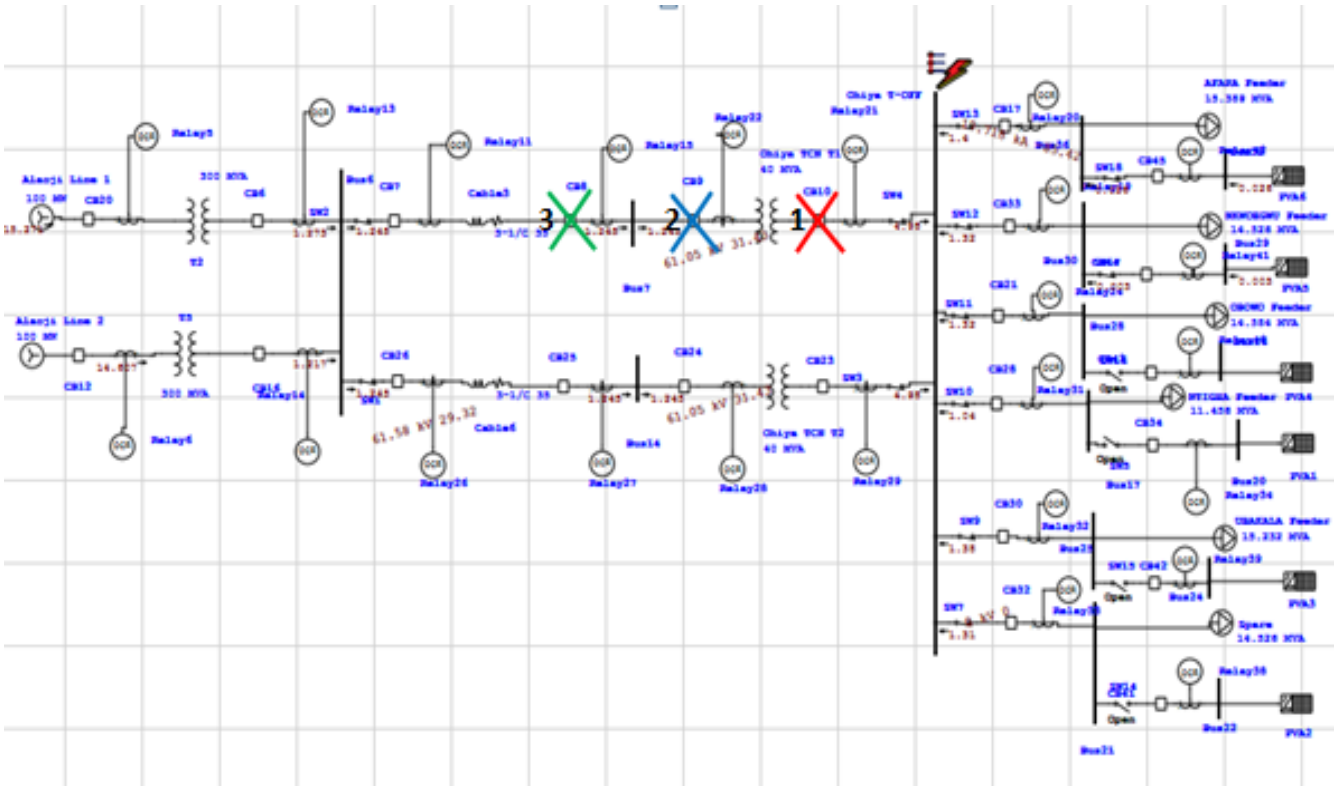

Figure 7: Network diagram for fault located at 33 kV bus with 20% DG Penetration

Table 6: Sequence of operation summary report for fault at 33kV bus with 20% DG Penetration

Symmetrical 3-Phase Fault at 33kV bus			
Time (ms)	**ID**	**If (kA)**	**Condition**
10.0	R21	3.941	Phase –OC1 – 50
78.1	R22	2.865	Overload Phase – Thermal
83.3	R15	2.869	Overload Phase – Thermal
310	Bus-bar CB		Tripped by R21 Phase – OC1 – 50
378	CB9		Tripped by R22 Overload Phase
378	CB8		Tripped by R15 Overload Phase
2324	R22	2.865	Phase – OC1 – 51
2332	R15	2.869	Phase – OC1 – 51

G. When fault was located at 33kV bus with 50% DG Penetration

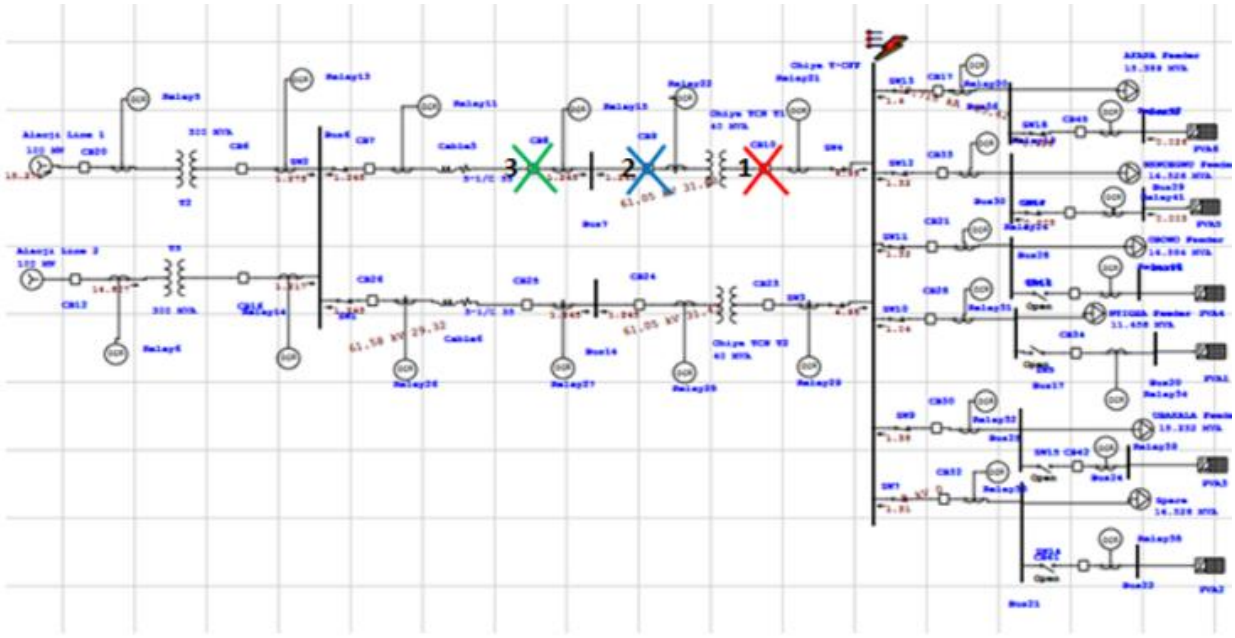

Figure 8: Network diagram for fault located at 33 kV bus with 50% DG Penetration

Table 7: Sequence of operation summary report for fault at 33kV bus with 50% DG Penetration

Symmetrical 3-Phase Fault at 33kV bus with 50% DG Penetration			
Time (ms)	**ID**	**If (kA)**	**Condition**
9.19	R21	4.091	Phase –OC1 – 50
77.2	R22	3.478	Overload Phase – Thermal
77.2	R15	3.479	Overload Phase – Thermal
303	Bus-bar CB		Tripped by R21 Phase – OC1 – 50
316	CB9		Tripped by R22 Overload Phase
319	CB8		Tripped by R15 Overload Phase
2312	R22	2.972	Phase – OC1 – 51
2314	R15	2.975	Phase – OC1 – 51

H. When fault was located at 33kV bus with 70% DG Penetration

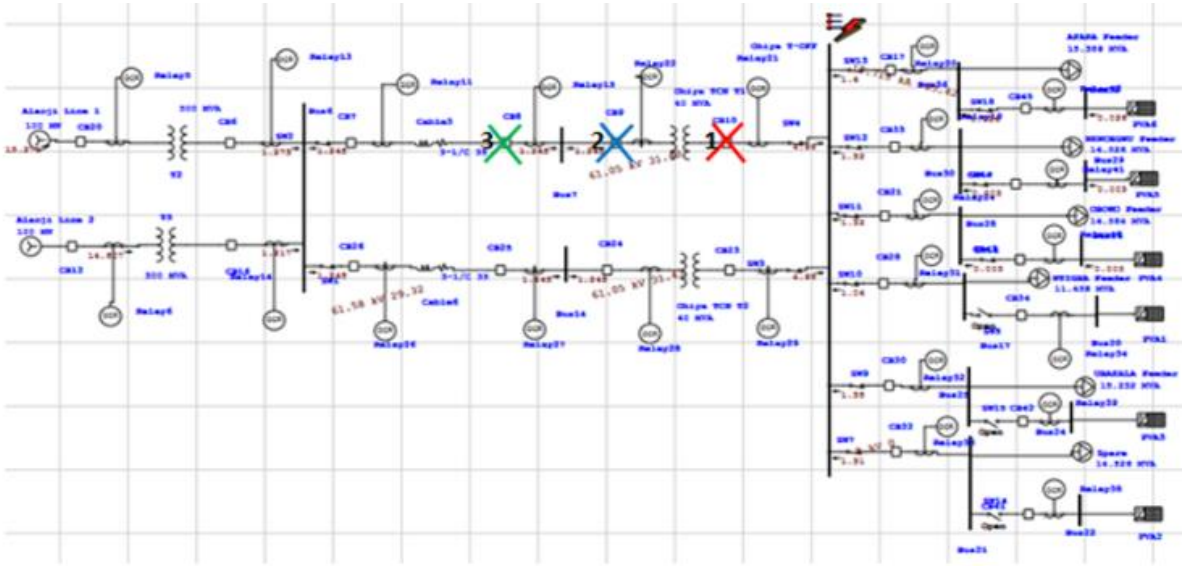

Figure 9: Network diagram for fault located at 33 kV bus with 70% DG Penetration

Table 8: Sequence of operation summary report for fault at 33kV bus with 70% DG Penetration

Symmetrical 3-Phase for fault at 33kV bus with 70% DG Penetration			
Time (ms)	**ID**	**If (kA)**	**Condition**
21.3	R21	1.248	Phase –OC1 – 50
125.3	R5	1.212	Overload Phase – Thermal
127.1	R6	1.185	Phase – OC1 – 50
524	CB10		Tripped by R20 Phase – OC1 – 50
529	CB20	1.250	Tripped by R21 Overload Phase
536	CB12	1.252	Tripped by R22 Phase – OC1 – 50

I. Case when fault is at 132kV side without DG

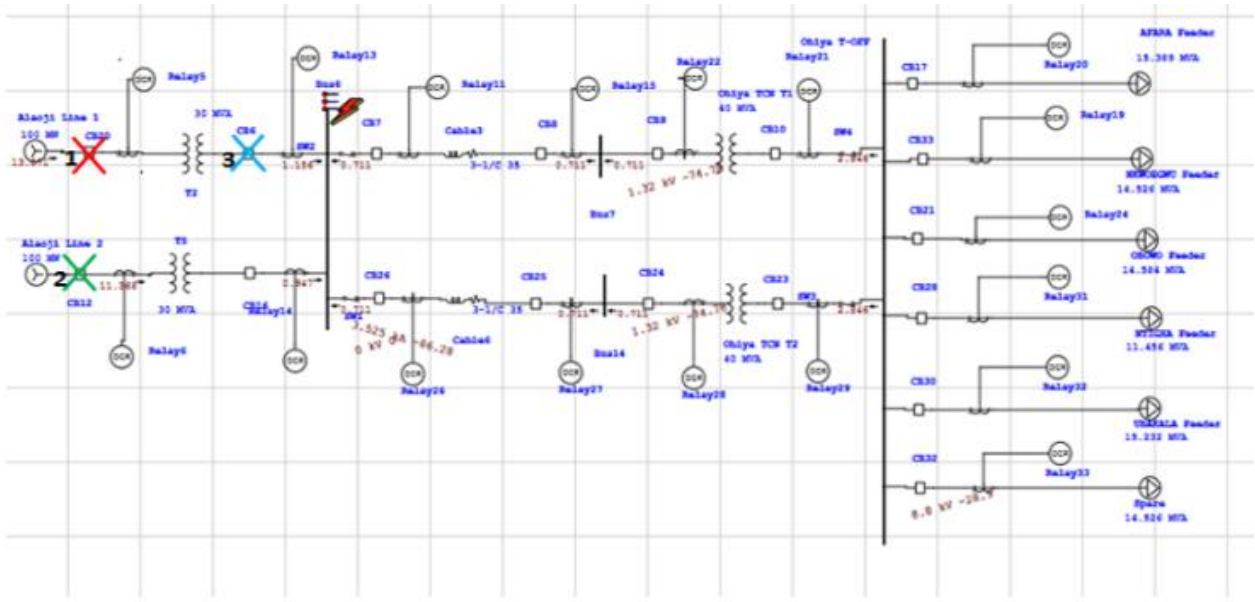

Figure 10: Relay coordination simulation for 132 kV side without DG

Table 9: Sequence of operation summary for fault at 132kV bus without DG

Symmetrical 3-Phase Fault at 132kV side			
Time (ms)	**ID**	**If (kA)**	**Condition**
153	R5	2.843	Phase –OC1 – 50
158	R6	2.839	Overload Phase – Thermal
285	R13	2.713	Overload Phase – Thermal
453	CB20		Tripped by R5 Phase – OC1 – 50
578	CB12		Tripped by R6 Overload Phase
610	CB6		Tripped by R13 Overload Phase
1124	R6	2.843	Phase – OC1 – 51
1132	R13	2.839	Phase – OC1 – 51

V. CONCLUSION

The sequence of operation result for fault at Afara feeder end, 33kV bus and 132kV side without DG showed that the relays picked the faults at good time, tripped the circuit breakers accurately and have correct relay tripping coordination. For increased level of DG penetration of 20%, the sequence of operation showed correct fault current measurement, accurate tripping time for the relays and correct coordination for the circuit breakers. When the level of DG penetration was increased to 50%, the tripping time of the relays were slightly delayed and affected due to lower values of fault current seen by the relays but no effect was found in the tripping coordination of the circuit breaker. In cases of higher DG penetration as found in 70% DG penetration, the sequence of operation results for faults at different locations showed that the system operated in islanded mode. All the simulation results for high level of penetration up to 70% the system can be seen to operate in islanded mode and the fault current was found to be substantially lower than the fault current for the system without DG or with low DG penetration. This resulted to the delay in tripping time and loss of relay coordination and the fault current was affected due to the high DG insertion in the distribution system. Thus, the results of the simulations can be affirmed that the location of fault bears no significance to the behaviour of the relays rather the level the DG penetration has a considerable affect on the fault current, relay tripping time and coordination.

REFERENCES

[1] B. Kroposki, B. Johnson, Y. Zhang, V. Gevorgian, P. Denholm, B. M. Hodge, B. M., & B Hannegan, (2017). Achieving a 100% Renewable Grid: Operating Electric Power Systems with Extremely High Levels of Variable Renewable Energy. IEEE Power and Energy Magazine, 15(2), 61-73.

[2] C. E Ezendiokwelu, O. A Ezechukwu & T. C Madueme, "Analysis of the Impact of Thyristor Controlled Series Capacitor on the Performance of Distance Relay," Iconic Research And Engineering Journal, 2(3), 2018, Pages 66-73.

[3] K. A. Wheeler, S. O. Faried & M. Elsamahy (2016). Assessment of distributed generation influences on fuse-recloser protection systems in radial distribution networks. Transmission and Distribution Conference and Exposition (T&D), 2016 IEEE/PES, 1-5.

[4] P. Mohammadi & S. Mehraeen (2017). Challenges of PV integration in low-voltage secondary networks. IEEE Transactions on Power Delivery, 32(1) 525-535.

[5] S. M. Madani (1999). Analysis and design of power system protections using graph theory. Technische Universiteit Eindhoven. https://doi.org/10.6100/IR523152

[6] S. M. Brahma & A. Girgis (2002). Microprocessor-based reclosing to coordinate fuse and recloser in a system with high penetration of distributed generation. IEEE Power Engineering Society Winter Meeting, 1(2) 453-458.

[7] I. C Okpara & C. O Ahiakwo (2021). Protection System Design for Power Distribution System in the Presence of Distributed Generation. International Journal of Communication System, 8(2), 1-16. http://doi.org/10.37591/RTECS

[8] N. Schaefer, T. Degner, A. Shustov, Keil T., & Jaeger J. (2010). Adaptive protection system for distribution networks with distributed energy resources. Fraunhofer IWES (formerly ISET e.V.), Germany, Koenigstor, 59(2), 1-5.

[9] M. Baran, & I. El-Markabi (2004). Adaptive over current protection for distribution feeders with distributed generators. Power Systems Conference and Exposition, 2004. IEEE PES, 2004, 715-719.

[10] P. Mahat, Z. Chen, B. Bak-Jensen & C. L Bak (2011). A simple adaptive overcurrent protection of distribution systems with distributed generation. IEEE Transactions on Smart Grid, 2(3), 428-437.

[11] H. Yazdanpanahi, Y. W Li & W. Xu (2012). A new control strategy to mitigate the impact of inverter-based DGs on protection system. IEEE Transactions on Smart grid, 3(3), 1427-1436.

[12] S. Shen (2017). An adaptive protection scheme for distribution systems with DGs based on optimized Thevenin equivalent parameters estimation. IEEE Transactions on Power Delivery, 32(1), 411-419.

[13] D. S Kumar, D. Srinivasan & T. Reindl (2016). A fast and scalable protection scheme for distribution networks with distributed generation. IEEE Transactions on Power Delivery, 31(1), 67-75.

[14] Y. Sheng, & S. M Rovnyak (2004). Decision tree-based methodology for high impedance fault detection. IEEE Transactions on Power Delivery, 19(2), 533-536.

[15] S. Samantaray & P. Dash (2010). High impedance fault detection in distribution feeders using extended kalman filter and support vector machine. International Transactions on Electrical Energy Systems, 20(3), 382-393.

[16] N. Hadjsaid, J. F Canard, & F. Dumas (1999). Dispersed generation impact on distribution networks. Computer Applications in Power, IEEE, 12(7), 22-28.